RSC Advances

ROYAL SOCIETY OF CHEMISTRY

www.rsc.org/advances

Journal Name

RSCPublishing

ARTICLE

Energetic performances of pure silica STF and MTT-type zeolites under high pressure water intrusion

Cite this: DOI: 10.1039/xoxxoooooox

A. Ryzhikov,[a] I. Khay,[a] H. Nouali,[a] T.J. Daou and J. Patarin[a]

Received ooth January 2012,
Accepted ooth January 2012

DOI: 10.1039/xoxxoooooox

www.rsc.org/

Experimental water intrusion–extrusion isotherms were performed at room temperature on two pure silica MTT- and STF-type hydrophobic zeolites (zeosils) with 1D channel and cage pore system, respectively by applying or releasing a high hydraulic pressure. These zeosils were obtained by hydrothermal synthesis in fluoride medium and characterized by structural and physicochemical methods before and after water intrusion. The system "MTT-type zeosil-water" displays a spring behavior with an intrusion pressure of 176 MPa and a stored energy of 5.3 $J.g^{-1}$. No influence of water intrusion on the structure of MTT-type zeosil was found. The "STF-type zeosil-water" system shows a combination of shock-absorber and bumper behavior in the first cycle with an intrusion pressure of 51 MPa. Nevertheless in the following cycles the system demonstrates a spring behavior with an intrusion pressure of 38 MPa. Such behavior can be explained by the formation of silanol groups under intrusion in some pores confirmed by NMR spectroscopy and TG data.

Introduction

Zeolites are microporous solids with a framework built from TO_4 tetrahedra (T=Si,Al) which form cages, channels and cavities. They are widely used in industrial catalysis, adsorption, molecular sieving and ion-exchange processes.[1] Among them pure silica zeolites (zeosils) prepared in fluoride medium present a high interest because of their hydrophobic properties which are useful for adsorption of non-polar organic compounds and also for potential applications in the energetic field. The first studies on energetic applications of zeosils were realized by our group in 2001.[2,3] This approach is based on high pressure intrusion of liquid water into the pores of zeosils, which are known to have hydrophobic properties. To penetrate water in the porous solid (intrusion), a certain pressure must be applied. Under intrusion liquid water is transformed into a multitude of molecular clusters in the pores. Thus, the supplied mechanical energy during the compression step is converted to interfacial energy. By reducing the pressure, the system can induce an expulsion of the liquid out of the pores of zeolite (extrusion). Depending on zeolite structure, the "zeosil−water" system is able to restore, dissipate, or absorb energy and therefore, it displays a spring, shock-absorber, or bumper behavior, respectively. Several pure-silica zeolites were studied for this process.[4-16] It was observed that the most part of "zeosil-water" systems behave as a spring or shock-absorber with small hysteresis. The structures such as *BEA[2] and IFR[10] show a bumper behavior with an irreversible water intrusion. The behavior of the systems and the values of intrusion pressure depend on physicochemical and topological parameters related to the zeolite framework such as hydrophobic/hydrophilic character, pore size, geometry and channel dimensionality. It was found that generally the channel-type zeolite structures led to considerably higher intrusion pressures than the cage-type ones with similar pore diameters. A summary of energetic performances of pure-silica zeolites with different crystalline structures was previously reported.[16-18]

This work focuses on the water intrusion-extrusion in pure silica STF and MTT-type zeolites and their characterization by powder X-ray diffraction, ^{29}Si NMR spectroscopy, thermogravimetric analysis in order to better understand the influence of structure parameters on the energetic performances. These zeolites are characterized by one-dimensional channel (MTT) and cage (STF) system with 10-member ring (MR) openings and pore size of 0.45-0.52 and 0.54-0.57 nm, respectively and have not been yet studied for energetic application.

Results and discussion

XRD and SEM Characterisations. The XRD patterns of MTT- and STF-type zeosil samples before and after water intrusion−extrusion of water are given in Figure 1. The patterns show a sequence of large and narrow diffraction peaks typical for the corresponding structures. These peaks were indexed in the triclinic and orthorhombic symmetry for STF- and MTT-type sample, respectively. The corresponding unit-cell parameters are reported in

Table 1. No significant change of the unit-cell parameters is observed after water intrusion-extrusion experiments, which means that at the long-range order, the STF and MTT structure, were not affected.
In the case of MTT-type zeosil traces of amorphous phase are observed at 20-25°, presence are confirmed by SEM and N_2 adsorption measurements (see below).

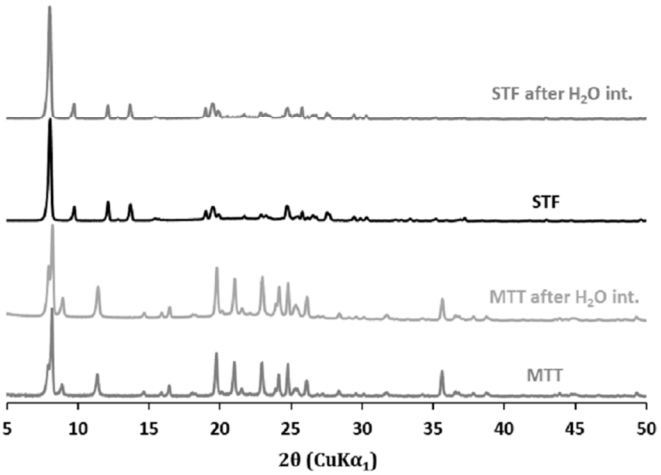

Figure 1. X-ray diffraction patterns of the MTT- and STF-zeosil samples before and after three water intrusion-extrusion cycles.

Table1. Unit-cell parameters of STF and MTT-type zeosil samples before and after three water intrusion−extrusion cycles.

Structure-type	STF-type zeosil	STF-type zeosil after intrusion-extrusion	MTT-type zeosil	MTT-type zeosil after intrusion-extrusion
a (Å)	11.456(8)	11.437(9)	21.559(11)	21.539(10)
b (Å)	11.558(9)	11.549(13)	11.182(12)	11.142(12)
c (Å)	7.399(7)	7.394(9)	5.039(20)	5.036(14)
V (Å^3)	1918(35)	1909(33)	1213.53(12)	1208.58(15)
α (°)	94.72(5)	94.79(6)	90	90
β (°)	95.89(5)	95.70(4)	90	90
γ (°)	104.84(4)	104.59(5)	90	90

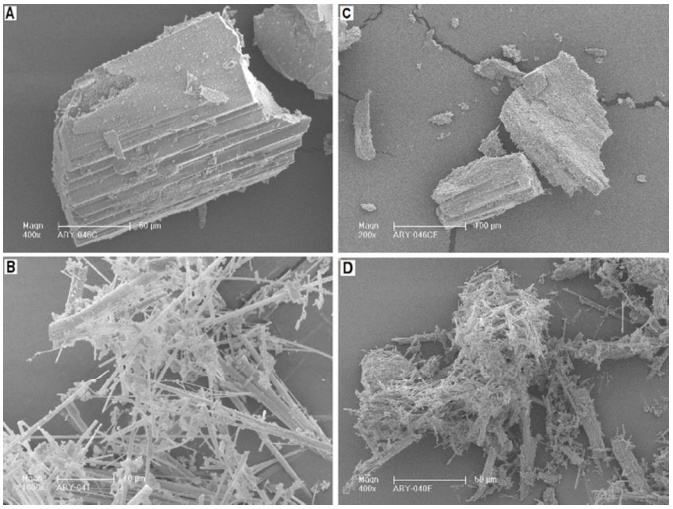

Figure 2. SEM micrographs of the STF-type and MTT-type zeosil samples before (a and b) and after (c and d) intrusion-extrusion experiments.

The crystal morphology of the STF- and MTT-type zeolites was examined by scanning electron microscopy. No difference between nonintruded and water-intruded samples was found. SEM images are presented in Figure 2. For STF-type zeosil large faceted crystals of irregular shape with a size ranging from 100 to 150 μm are observed (Figure 2a,c). The MTT-type zeosil is composed from long rod-shaped crystals with a length from several to several tens microns and a diameter of 0.3 to 2 μm, a presence of small aggregates probably ascribed to amorphous phase is also observed (Figure 2b,d).

N_2 Adsorption−Desorption Isotherms. The N_2 adsorption−desorption isotherms of the nonintruded and intruded STF- and MTT- type zeosil samples are shown in Figure 3. The isotherm of STF-type sample is mainly of type I characteristic of microporous solids. The BET surface area and microporous volume of the nonintruded STF-type zeosil are equal to 296 $m^2.g^{-1}$ and 0.11 $cm^3.g^{-1}$, respectively. For the water intruded-extruded sample the values of BET surface area and pore volume drop drastically to 9 $m^2.g^{-1}$ and close to 0 $cm^3.g^{-1}$. Therefore, although the structure is preserved from XRD analysis, after such an experiment the access of N_2 molecules to the porosity is completely blocked. It can be supposed that silanol groups, in spite of their low concentration (0.15 OH group per unit cell, see below TG measurements), are formed in the pore openings. It has to be noted that water molecules adsorbed on these silanol groups are probably still present. Indeed, the activation temperature of the samples for the N_2 adsorption-desorption measurements was 90 °C under vacuum (see experimental section) and according to the TG experiments, the removal of these water molecules occurs between 200-250 °C. The isotherm of MTT-type zeosil shows the presence of mesoporosity at high relative pressure ($p/p° > 0.8$) values. The values of BET surface area and microporous volume are particularly low: 81 $m^2.g^{-1}$ and ~0.03 $cm^3.g^{-1}$, respectively. After the intrusion-extrusion experiments these values decrease to 40 $m^2.g^{-1}$ and ~0.01 $cm^3.g^{-1}$. Similar results were observed for the TON-type zeosil which displays a similar one-dimensional channel structure.[12] It can be supposed that for these two zeosils, the surface area and pore volume are underestimated because nitrogen molecules cannot completely fill the 10-MR channels running along the [100] crystallographic direction and the growing axis of rod-shaped crystals. Using molecular probes Myers estimated that the pore volume of TON-type zeosil is about 0.07 $cm^3.g^{-1}$.[19] The mesoporosity in MTT-type zeosil can be related with the presence of porous amorphous phase in the sample.

Thermal Analysis. The experimental results issued from the thermogravimetric (TG) analysis of STF and MTT-type zeosil samples before and after intrusion-extrusion experiments are depicted in Figure 4. The total weight loss of the nonintruded samples of STF-type zeosil is very low (0.18%) and principally attributed to physisorbed water. Thus, the highly hydrophobic character of STF-type zeosil is confirmed. After water intrusion the total weight loss increases up to 0.55 % and three weight loss steps are clearly observed. The first one (0.18 wt %), located between 30 and 170 °C, is ascribed to the desorption of physisorbed water molecules. The second step of 0.16 wt %, located at 170-320 °C, can be attributed to the removal of water molecules adsorbed on silanol groups, and the third one (0.13 wt %, 510°-670°C) to the removal of water molecules arising from dehydroxylation reactions. The last step of weight loss corresponds to 0.15 OH group per unit cell ($Si_{16}O_{32}$). It can be concluded that a small amount of silanol defects is formed under water intrusion.

For MTT-type zeosil the thermogravimetric curves before and after water intrusion are very similar. As for the STF-type zeosil the weight loss (1.1 wt %) between 30 and 170°C corresponds to physisorbed water desorption. This step is followed by continuous weight loss from 200° to 800°C that can be ascribed to the desorption of chemisorbed water molecules and the removal of silanol groups. In the case of water-intruded sample, the value of the weight loss (0.74 wt %) is slightly higher than that of the nonintruded MTT-type zeosil (0.69 wt %). This difference corresponds to 0.08 OH group per unit cell.

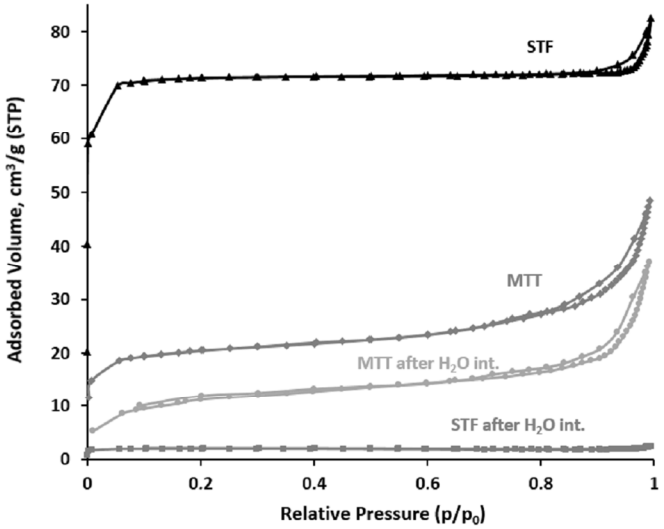

Figure 3. N_2 adsorption−desorption isotherms at -196 °C of the STF and MTT-type zeosil samples before and after three water intrusion-extrusion cycles.

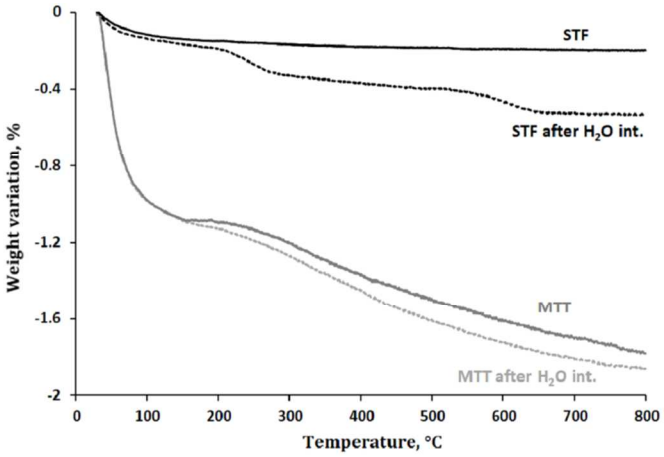

Figure 4. TG curves of STF and MTT-type zeosil samples before and after three water intrusion-extrusion cycles.

^{29}Si MAS NMR Spectroscopy. The ^{29}Si MAS NMR spectra of the MTT and STF-zeosils before and after water intrusion−extrusion experiments are shown in Figure 5. The spectrum of the nonintruded STF-type sample exhibits 6 main resonances in the -107 to -117 ppm range ascribed to the non equivalent crystallographic silicon Q_4 ($Si(OSi)_4$) sites. After three water intrusion-extrusion cycles the spectrum change slightly: the main six resonances overlap more and new resonances of very low intensity appear in the -97 to -100 ppm range. The last ones can be assigned to Q_3 groups corresponding to defects such as Si-OH groups.

The spectrum of MTT-type zeosil exhibits five main resonances in the range of -108 to -118 ppm, which can be attributed to Q_4 silicon sites. After water intrusion-extrusion experiments the spectrum does not change, only a slight broadening of the resonances is observed.

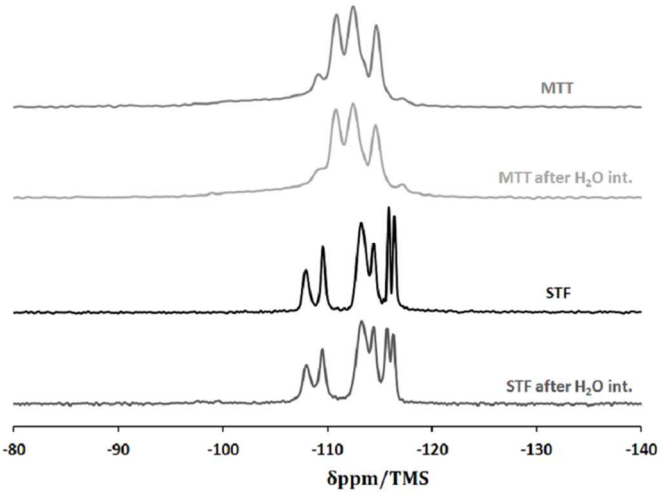

Figure 5. ^{29}Si−MAS NMR spectra of the MTT and STF-zeosil samples before and after three water intrusion-extrusion cycles.

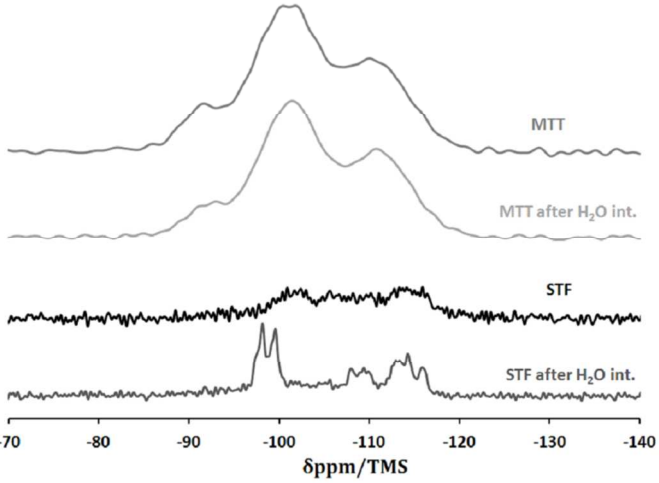

Figure 6. ^{1}H−^{29}Si CPMAS NMR spectra of the MTT and STF-zeosil samples before and after three water intrusion-extrusion cycles

^{1}H−^{29}Si CPMAS NMR Spectroscopy. The ^{1}H−^{29}Si CPMAS NMR spectra of the MTT and STF-zeosils before and after water intrusion−extrusion experiments are shown in Figure 6. These spectra were performed in order to enhance the silicon atoms that bear protons and thus to get evidence of the presence of silanol groups. Under these NMR experimental conditions (short contact time), the spectra of the nonintruded and intruded MTT-type zeosil are very similar. Three main broad resonances are observed at -92, -101 and -111 ppm, which can be attributed to Q_2, Q_3 and Q_4 sites, respectively. The presence of Q_2 ($(HO)_2Si(OSi)_2$) groups is quite surprising. This latter component might also correspond to the amorphous silica particles observed by SEM. An absence of

significant changes in NMR spectra of MTT-type zeosil is in agreement with the TG results.

The $^{1}H-^{29}Si$ CPMAS NMR spectrum of the nonintruded STF-type zeosil displays only a very broad and low signal which indicates the absence of defect sites. After water intrusion-extrusion experiments, two weak resonances at -98 and -100 ppm corresponding to Q_3 sites appear on the NMR spectrum. Thus, in agreement with the TG results, the formation of a small amount of silanol ($Si-(OSi)_3OH$) groups arising from the breaking of siloxane bridges under water intrusion is clearly evidenced.

^{1}H-MAS NMR. The ^{1}H-MAS NMR spectra of the MTT and STF-zeosils before and after water intrusion−extrusion experiments are shown in Figure 7. The ^{1}H-MAS NMR allows to characterize the hydrogenated species in silicates. In the case of MTT-type zeosil before and after water intrusion-extrusion experiment a resonance is observed at 4.3 ppm with an additional small resonance at 0.8 ppm. The first one is characteristic to water adsorbed molecules, the second one can be assigned to the protons of silanol groups (≡Si–OH).[20] The intensity of the resonance is higher for the intruded sample, which means that the adsorbed water amount is greater in this case.

On the spectrum of the nonintruded STF-type zeosil sample a large resonance at 4.1 ppm with an additional one at 4.5 ppm is observed. After water intrusion-intrusion the spectrum change considerably. Two main broad resonances at 4.6 and 3.1 ppm ascribed to the protons of adsorbed water molecules are observed. Also two small double resonances at 1.1-1.0 and -0.08 - -0.24 ppm ascribed to silanol groups appear. Thus, the formation of silanol groups under intrusion is clearly confirmed.

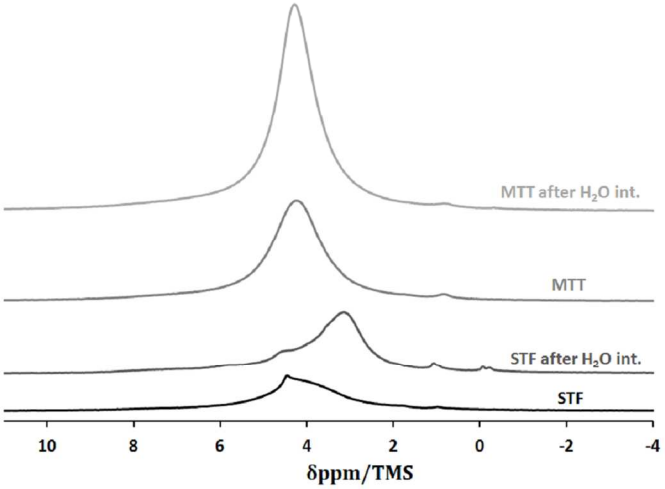

Figure 7. ^{1}H−MAS NMR spectra of the MTT and STF-zeosil samples before and after three water intrusion-extrusion cycles.

Intrusion−Extrusion Isotherms. The pressure−volume diagrams of the "STF-type zeosil – water" and the "MTT-type zeosil – water" systems are shown in Figure 8. The corresponding data are reported in Table 2. Three intrusion-extrusion cycles were performed for each experiment. As it was shown in previous works, the volume variation observed at low pressure (< 1 MPa) corresponds to the compression and the liquid filling in the interparticular porosity of the zeolitic pellet.[14,15] Contrary to the BET results, the water intrusion in the MTT-type zeosil is observed, thus the pore volume is accessible to water molecules. The ''MTT zeosil–water'' system displays a spring behavior. After 1, 2 and 3 intrusion–extrusion cycles, the extrusion and the extrusion curves are completely superimposable. Therefore for a better clarity, only the first cycle is reported in Figure 8. In all cases, an important spread of the intrusion step is observed. The intrusion of water starts at ~120 MPa with a full filling of the pores at around ~230 MPa. The average value for the intrusion pressure is reached at P_{int} = 176 MPa and at 174 MPa for the extrusion pressure (P_{ext}). Such a value for the intrusion pressure is one of highest ones among all studied "zeolites-water" systems. The highest values were observed for TON-type zeosil (180 MPa)[12] and ITW (172 MPa).[15] It should be noticed that the MTT and TON structures are similar and display an unidimensionnal channel system with 10 MR openings. The value of the water intruded volume in MTT-type zeosil is close to 0.03 $mL.g^{-1}$. The "MTT-type zeosil-water" system can restore 99% of the stored energy which is about 5.3 $J.g^{-1}$. The spring behavior is correlated with an absence of silanol defects observed in RMN and TG experiments. It should be noticed that the values of intruded volume and stored energy for MTT-type zeosil are underestimated because of the presence of amorphous phase.

STF-type zeosil demonstrates a difference between the first intrusion-extrusion cycle and the following ones. The first and the second intrusion-extrusion cycles are shown in Figure 8. In the first cycle the "STF-type zeosil-water" system shows a combination of shock-absorber and bumper behavior. The intrusion and extrusion of water occurs at 51 MPa and 37 MPa, respectively, but all the liquid is not expelled from the solid. The intruded volume in the STF-type zeosil is close to 0.04 $mL.g^{-1}$, whereas the extruded one is 0.03 $mL.g^{-1}$. Therefore the nonextruded liquid is close to 0.01 $mL.g^{-1}$. It can be supposed that during the intrusion step, silanol groups as confirmed by ^{29}Si NMR and TG measurements (0.15 OH group per unit cell) are formed and part of the intruded water molecules are adsorbed on them. The second and third intrusion-extrusion cycles are identical; the system demonstrates a spring behavior with an intrusion pressure of 38 MPa and a stored energy of 1.1 $J.g^{-1}$. Such a water intrusion-extrusion behavior was already observed for the CHA-type zeosil which is also a cage-type zeosil[6,9]; after the first cycle part of the liquid is still present in the solid, whereas for the other cycles a completely reversible process is observed.

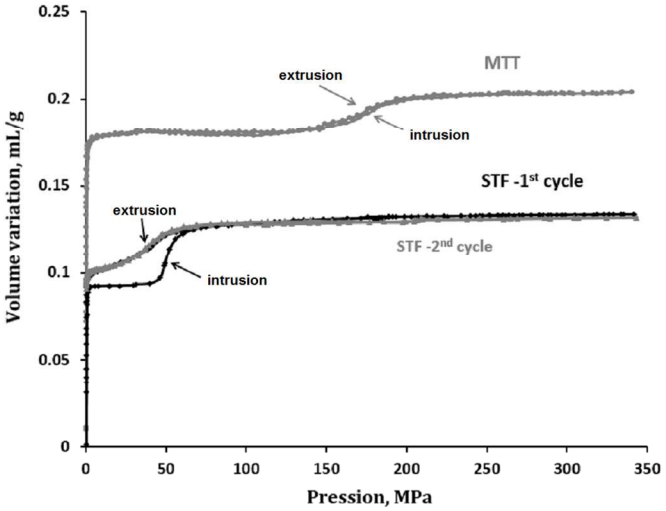

Figure 8. The first intrusion-extrusion cycle of the "MTT-type zeosil–water" system and the first two cycles of the "STF-type zeosil-water"system. For a better visibility, the diagrams are shifted along the Y-axis.

The value of the intruded volume (0.04 $mL.g^{-1}$ in the 1st cycle) is lower than the one obtained from N_2 adsorption-desorption isotherms (0.11 $mL.g^{-1}$). However it was shown by Desbiens *et al.* that the computed water density in MFI zeolite structure is approximately 0.6 $g.mL^{-1}$.[5] In our case this value is lower, that could be related with different arrangements of water clusters into the pores of STF structure.

The case of MTT and STF-type zeolites confirms again the observation that channel-type zeosils show considerably higher intrusion pressure of water than the cage-type ones.[16] The intrusion pressure value for STF-type zeosil with cage-type structure is in the same order than ones of other cage-type zeolites studied in our group: CHA[9], STT[13], whereas the intrusion pressure in MTT-type zeosil is close to the values observed for channel type zeosil with 8 and 10 MR openings: FER[8], TON[12], ITW[15].

Table 2. Characteristics of the "MTT- and STF-type zeosil - water" systems: intrusion (P_{int}) and extrusion (P_{ext}) pressures, intruded (V_{int}) and extruded (V_{ext}) volumes, stored (E_s) and restored (E_r) energies and the energy yield.

	STF-type zeosil	MTT-type zeosil
P_{int} [a] (MPa)	51*/38**	176
V_{int} [a] (mL/g)	0.04*/0.03**	0.03
P_{ext} [a] (MPa)	37	174
V_{ext} [a] (mL/g)	0.03	0.03
E_s [b] (J/g)	1.15**	7
E_r [c] (J/g)	1.1	5.3
Yield (%)	96**	99
Behavior	Bumper-shock absorber*, Spring**	Spring

(a) determined from intrusion−extrusion isotherms
(b) stored energy Es = V_{int} x P_{int}
(c) restored energy Er = V_{ext} x P_{ext}
* -1st cycle, ** - 2nd and 3d cycles.

Experimental

STF-type zeolite was synthesized in fluoride medium according to a procedure similar to that described in reference.[21] The synthesis requires the presence of 6,10-diméthyl-5-azoniaspiro[4,5]decane hydroxide (DMASD) as a structure-directing agent prepared in the laboratory. Tetraethoxysilane (TEOS, Aldrich, 98%) was used as the silica source. The reaction gel had the following molar composition: 1 SiO_2 : 0.25 DMASD : 0.25 HF (40%, Normapur) : 5 H_2O. The mixture, transferred into a PTFE-lined stainless-steel autoclave, was heated at 150 °C for 14 days. MTT-type zeolite was also synthesized in fluoride medium. The synthesis requires the presence of dipropylamine (DPA) as structure-directing agent (55% solution of DPA, Aldrich). Ludox HS-30 (Aldrich, 98%) was used as the silica source. The reaction gel had the following molar composition: 1 SiO_2 : 5 DPA : 5 HF (40%, Normapur) : 30 H_2O. The mixture, transferred into a PTFE-lined stainless-steel autoclave, was heated at 170 °C for 30 days. After synthesis, the solids were calcined under air at 900 °C during 5 hours for MTT-type zeosil and at 550°C during 6 hours and 800°C during 5 h for STF structure in order to remove the organic template.

X-ray diffraction patterns of the different samples were recorded in a Debye−Scherrer geometry on a STOE STADI-P diffractometer equipped with a curved germanium (111), primary monochromator, and a linear position-sensitive detector (6° 2θ) using Cu $K\alpha_1$ radiation (λ = 0.15406 nm). Measurements were achieved for 2θ angle values in the 3−50 range, step 0.15° 2θ, and time/step = 120 s. The unit-cell parameters were determined using Louër's DICVOL91 indexing routine[22] of the STOE WinXPOW program package.[23]

The size and the morphology of the crystals were determined by scanning electron microscopy (SEM) using a Philips XL 30 FEG microscope.

Nitrogen adsorption−desorption isotherms were performed at -196 °C using a Micromeritics ASAP 2420 apparatus. Prior to the adsorption measurements, the samples were outgassed at 90°C overnight under vacuum to eliminate physisorbed water. Low degassing temperature was chosen to avoid the dehydroxylation process. The specific surface area (S_{BET}) and microporous volume (V_{micro}) were calculated using the BET and t-plot methods, respectively.

Thermogravimetric (TG) analyses were carried out on a TG/DSC Mettler Toledo STARe system apparatus, under air flow, with a heating rate of 5 °C/min from 30 to 800 °C.

^1H MAS, ^{29}Si MAS and ^1H–^{29}Si CPMAS NMR spectra were recorded on a Bruker Advance II 300 MHz spectrometer, with a double-channel 7 mm Bruker MAS probe. The recording conditions are given in Table 3.

Table 3. Recording Conditions of the ^1H MAS, ^{29}Si MAS and ^1H–^{29}Si CPMAS NMR Spectra.

	^1H	^{29}Si	
	MAS	MAS	CP MAS
Chemical shift standard	TMS[a]	TMS[a]	TMS[a]
Frequency (MHz)	300.07	59.6	59.6
Pulse width (μs)	5.06	1.87	4
Flip angle	π/2	π/6	π/2

Contact time (ms)	/	/	8
Recycle time (s)	10[b]	80	10[b]
Spinning rate (kHz)	4	4	4
Scans number	8	1000	16000

[a] TMS : TetraMethylSilane

[b] The relaxation time t_1 was optimized

The water intrusion−extrusion experiments in the zeosil samples in the form of compressed pellets were performed at room temperature using a modified mercury porosimeter (Micromeritics Model Autopore IV), as described in our previous works.[15] Before these experiments, the pellets were outgassed at 300 °C under vacuum. The values of the intrusion (P_{int}) and extrusion (P_{ext}) pressures correspond to that of the half volume total variation. The pressure is expressed in megapascals (MPa) and the volume variation in milliliters (mL) per gram of outgassed samples. The experimental error is estimated to 1 % on the pressure and on the volume. After intrusion-extrusion experiments the samples were dried at 70 °C overnight, and hydrated in 80 % relative humidity atmosphere during 24 h in order to set the hydration state.

Conclusions

The energetic performances of pure silica MTT and STF-type zeosils in water intrusion−extrusion experiments were studied. These zeosils are characterized by one-dimensional channel (MTT) and cage (STF) system 10-member ring (MR) openings. The "MTT-type zeosil- water" system shows a spring behavior with average values for the intrusion pressure of 176 MPa and stored energy of 5.3 $J.g^{-1}$. No influence of water intrusion on the structure of MTT-type zeosil was found. The "STF-type zeosil-water" system shows a combination of shock-absorber and bumper behavior in the first cycle with intrusion pressure of 51 MPa and partially irreversible water extrusion. In the following cycles the system demonstrates a spring behavior with the intrusion pressure of 38 MPa and a stored energy of 1.1 $J.g^{-1}$. Such behavior can be explained by a formation of Q_3 silanol groups arising from the breaking of siloxane bridges under intrusion, that is confirmed by ^{29}Si NMR spectroscopy and TG data. The values obtained for MTT and STF-type zeosils confirm the hypothesis that the channel-type zeosils show considerably higher intrusion pressure of water than the cage-type ones.

Acknowledgements

The authors would like to thank Dr. S. Rigolet for fruitful discussions.

Notes and references

Université de Haute Alsace (UHA), CNRS, Equipe Matériaux à Porosité Contrôlée (MPC), Institut de Science des Matériaux de Mulhouse (IS2M), UMR 7361, ENSCMu, 3 bis rue Alfred Werner, F-68093 Mulhouse, France.
E-mail: andrey.ryzhikov@uha.fr; joel.patarin@uha.fr

1 J. Čejka, H. Van Bekkum, A. Corma and F. Schüth, *Stud. Surf. Sci. Catal.,* 2007, **168**, 525.
2 V. Eroshenko, R. C. Regis, M. Soulard and J. Patarin, *J. Am. Chem. Soc.,* 2001, **123**, 8129.
3 V. Eroshenko, R. C. Regis, M. Soulard and J. Patarin, *C. R. Phys*., 2002, **3**, 111.
4 M. Soulard, J. Patarin, V. Eroshenko and R. Regis, *Stud. Surf. Sci. Catal.,* **2004**, *154B*, 1830.
5 N. Desbiens, I. Demachy, A. Fuchs, H. Kirsh-Rodeschini, M. Soulard and J. Patarin, *Angew. Chem., Int. Ed.,* 2005, **44**, 5310.
6 M. Trzpit, M. Soulard and J. Patarin, *Chem. Lett.,* 2007, **36**, 980.
7 M. Trzpit, M. Soulard, J. Patarin, N. Desbiens, F. Cailliez, A. Boutin, I. Demachy and A. Fuchs, *Langmuir*, 2007, **23**, 10131.
8 F. Cailliez, M. Trzpit, M. Soulard, I. Demachy, A. Boutin, J. Patarin and A. Fuchs, *Phys. Chem. Chem. Phys.,* 2008, **10**, 4817.
9 M. Trzpit, S. Rigolet, J.-L. Paillaud, C. Marichal, M. Soulard and J. Patarin, *J. Phys. Chem. B,* 2008, **112**, 7257.
10 M.-A. Saada, S. Rigolet, J.-L. Paillaud, N. Bats, M. Soulard and J. Patarin, *J. Phys. Chem. C,* 2010, **114**, 11650.
11 M.-A. Saada, M. Soulard, B. Marler, H. Gies and J. Patarin, *J. Phys. Chem. C,* 2011, **115**, 425.
12 L. Tzanis, M. Trzpit, M. Soulard and J. Patarin, *Microporous Mesoporous Mater.,* 2011, **146**, 119.
13 L. Tzanis, M. Trzpit, M. Soulard and J. Patarin, *J. Phys. Chem. C,* 2012, **116**, 4802.
14 L. Tzanis, B. Marler, H. Gies, M. Soulard and J. Patarin, *J. Phys. Chem. C,* 2013, **117**, 4098.
15 I. Khay, L. Tzanis, T. J. Daou, H. Nouali, A. Ryzhikov and J. Patarin, *Phys. Chem. Chem. Phys.,* 2013, **15**, 20320**.**
16 L. Tzanis, M. Trzpit, M. Soulard and J. Patarin, *J. Phys. Chem. C,* 2012, **116**, 20389.
17 L. Tzanis, H. Nouali, T. J. Daou, M. Soulard and J. Patarin, *J. Mater. Lett.,* 2014, **115**, 229.
18 I. Khay, T. J. Daou, H. Nouali, A. Ryzhikov, S. Rigolet and J. Patarin, *J. Phys. Chem. C*, 2014, **118**, 3935.
19 A. L. Myers, *Colloids Surf. A*, 2004, **241**, 9.
20 A. Burneau, J.-P. Gallas, in The Surface Properties of Silicas; Legrand, A. P., Ed.; John Wiley & Sons: Chichester, U.K., 1998, 145.
21 J.-L. Paillaud, B. Harbuzaru, J. Patarin, *Microporous Mesoporous Mater.,* 2007, **105**, 89.
22 A. Boultif and D. Louër, *J. Appl. Crystallogr.*, 1991, **24**, 987.
23 STOE WinXPOW, version 1.06; STOE and Cie: Darmstadt, Germany, 1999.

